SNARE-Driven, 25-Millisecond Vesicle Fusion In Vitro

Tingting Liu,* Ward C. Tucker,† Akhil Bhalla,† Edwin R. Chapman,† and James C. Weisshaar‡
Departments of *‡Chemistry and †Physiology, University of Wisconsin-Madison, Madison, Wisconsin 53706

ABSTRACT Docking and fusion of single proteoliposomes reconstituted with full-length v-SNAREs (synaptobrevin) into planar lipid bilayers containing binary t-SNAREs (anchored syntaxin associated with SNAP25) was observed in real time by wide-field fluorescence microscopy. This enabled separate measurement of the docking rate k_{dock} and the unimolecular fusion rate k_{fus}. On low t-SNARE-density bilayers at 37°C, docking is efficient: $k_{dock} = 2.2 \times 10^7\ M^{-1}\ s^{-1}$, ~40% of the estimated diffusion limited rate. Full vesicle fusion is observed as a prompt increase in fluorescence intensity from labeled lipids, immediately followed by outward radial diffusion ($D_{lipid} = 0.6\ \mu m^2\ s^{-1}$); ~80% of the docked vesicles fuse promptly as a homogeneous subpopulation with $k_{fus} = 40 \pm 15\ s^{-1}$ ($\tau_{fus} = 25$ ms). This is 10^3–10^4 times faster than previous in vitro fusion assays. Complete lipid mixing occurs in <15 ms. Both the v-SNARE and the t-SNARE are necessary for efficient docking and fast fusion, but Ca^{2+} is not. Docking and fusion were quantitatively similar on syntaxin-only bilayers lacking SNAP25. At present, in vitro fusion driven by SNARE complexes alone remains ~40 times slower than the fastest, submillisecond presynaptic vesicle population response.

INTRODUCTION

Neurotransmitters are released by Ca^{2+}-triggered exocytosis, in which a 50-nm diameter synaptic vesicle fuses its lipid bilayer with that of the plasma membrane and releases its contents to the cell exterior (1–3). In neurons, triggered exocytosis occurs on submillisecond timescales after the onset of Ca^{2+} influx, implying that the key steps must involve rearrangement of local proteins and lipids (1,4). A variety of proteins, both cytoplasmic and membrane-anchored, are known to be critical to proper function of the Ca^{2+}-triggered fusion machinery (5,6). Fusion sites include one or more SNARE complexes (''soluble *N*-ethylmaleimide-sensitive factor attachment protein receptor'' complexes) (7). The internal structure of the cytoplasmic domain of a SNARE complex is known from crystallographic (8) and NMR studies (9,10). Each SNARE complex comprises a four-helix bundle. One helix is carried by synaptobrevin (syb, also called VAMP-2 or the v-SNARE protein), which is anchored in the vesicle membrane. The other three are carried by a binary complex between syntaxin (syx) and SNAP25 (here the ''binary t-SNARE''), with syx anchored in the plasma membrane. Accumulating evidence indicates that the Ca^{2+} sensor is a fourth protein called synaptotagmin (syt), which is anchored in the vesicle (5,11–15).

For the much simpler case of in vitro fusion of protein-free vesicles in solution phase, a free-energy barrier arises from the need to disrupt favorable hydrophobic lipid-lipid and hydrophilic lipid-water contacts at intermediate geometries (16,17). Certain peptides act as fusagens (18) by lowering the barrier. Recent evidence suggests that the SNARE protein anchors may create a channel through which neurotransmitters emerge (19), possibly before complete lipid mixing.

A reconstituted model system for Ca^{2+}-triggered exocytosis in principle provides a powerful tool allowing study of the structure and dynamics of vesicle-bilayer complexes as key components are added or subtracted one by one. The first reconstitution studies involved vesicle-vesicle fusion in bulk mixtures detected by dequenching of fluorescence from lipid-based probes. In groundbreaking work, Weber, Rothman, and co-workers showed SNARE-dependent fusion between vesicles reconstituted with syb and vesicles reconstituted with preformed syx/SNAP25 complexes (20,21). Fusion occurred slowly, on a timescale of tens of minutes, and fusion was not regulated by Ca^{2+}. Inclusion of full-length syt in the v-SNARE vesicles enhanced the fusion rate, but there was no Ca^{2+} dependence (22). A truncation of syx lacking the N-terminal H_{abc} region enhanced the fusion rate moderately (23). Tucker, Weber, and Chapman demonstrated SNARE-dependent fusion that was strongly enhanced on addition of Ca^{2+} and the cytoplasmic domain of syt (C2A-C2B, here C2AB), but fusion remained slow (24). Evidently, the minimal Ca^{2+}-triggered fusion system comprises SNARE complexes plus syt. In all such bulk fusion assays, the slow overall fusion rate could arise from inefficient docking of the vesicles to each other or inefficient subsequent fusion.

Throughout this article, we use docking in its generic sense of stable binding of two vesicles to each other or of a vesicle to an adsorption site on a planar bilayer. Docking or tethering of synaptic vesicles to fusion sites at the plasma membrane in vivo almost surely involves proteins in addition to the SNARE components under study here (25,26).

In the more recent vesicle-planar bilayer fusion assays (27,28), fluorescently labeled v-SNARE vesicles interact with a planar lipid bilayer supported on glass and

Submitted March 9, 2005, and accepted for publication June 14, 2005.

Address reprint requests to James C. Weisshaar, E-mail: weisshaar@chem.wisc.edu.

0006-3495/05/10/2458/15 $2.00

doi: 10.1529/biophysj.105.062539

containing preformed binary t-SNARE complexes. Wide-field fluorescence microscopy enables direct observation of individual docking and fusion events as they occur in real time. This enables independent measurement of the intrinsic docking rate constant k_{dock} and of the unimolecular rate of fusion k_{fus}, as first demonstrated here, to our knowledge. Two recent studies used the single-vesicle method to quantify vesicle fusion kinetics, with quite different results. Simon and co-workers formed t-SNARE planar bilayers on glass by vesicle fusion (28). The v-SNARE vesicles docked to the bilayer in the absence of Ca^{2+} but fused only rarely (0.35% fusion probability in 50 s). Addition of 100 μM Ca^{2+} (or Mg^{2+}) stimulated fusion of ~15% (or 4%) of the docked vesicles in 50 s, much faster than in the earlier vesicle-vesicle assays. However, there is no physiological evidence that Mg^{2+} should stimulate fusion. Brunger, Chu, and co-workers developed an analogous assay using bilayers containing a low number density of binary t-SNAREs or of syx alone (no SNAP25) (27). The observed fusion of docked vesicles was thermally driven by laser heating. The population decay time was ~20 s. Surprisingly, the presence or absence of SNAP25 had little effect on the fusion probability or timescale.

This work illustrates the full power of the single-vesicle methodology to separate docking and fusion kinetics. Using the same materials as in the Tucker-Chapman vesicle-vesicle assay (24) but with low t-SNARE copy number and low v-SNARE vesicle concentration, we observe efficient, SNARE-dependent docking followed by remarkably fast, Ca^{2+}-independent fusion. The rate constant for formation of a SNARE complex by close v-SNARE/t-SNARE encounters is $k_{dock} = (2.2 \pm 0.4) \times 10^7\ M^{-1}\ s^{-1}$, only three times smaller than the estimated diffusion-limited rate constant. Using a fast camera mode (5 ms/frame), we find that 80% of the docked vesicles undergo homogeneous, unimolecular fusion with $k_{fus} = 40 \pm 15\ s^{-1}$ at 37°C; ~65% of all docked vesicles fuse <25 ms after docking. This fusion rate is ~1000 times faster than observed in the two earlier single-vesicle assays. It is ~10^4 times faster than the fusion rate estimated for vesicle-vesicle assays under the assumption that fusion, not docking, is rate limiting.

Docking on t-SNARE bilayers is completely blocked by preincubation of the v-SNARE vesicles with the cytoplasmic domain of the binary t-SNARE complex and by preincubation of the binary t-SNARE bilayer with the cytoplasmic domain of the v-SNARE. Evidently, formation of *trans* SNARE complexes in the absence of syt and other regulatory cofactors can drive fusion on a 25-ms timescale. Syntaxin-only bilayers lacking SNAP25 yielded docking and fusion rate constants indistinguishable from the binary t-SNARE bilayers. In vitro fusion driven by ternary SNAREs in the absence of Ca^{2+}, syt, and other auxiliary proteins at present remains ~40 times slower than the fastest population decay of readily releasable vesicle in vivo (29).

MATERIALS AND METHODS

Protein expression and reconstitution into proteoliposomes

Proteins are expressed, purified, and reconstituted into vesicles as described previously (24). The specific proteins include: mouse synaptobrevin-2, here referred to as syb; the cytoplasmic domain of synaptobrevin $syb_{1–94}$ (residues 1–94); the full-length binary t-SNARE complex composed of rat syntaxin 1A (syx) and mouse SNAP25B; the cytoplasmic domain of the binary t-SNARE complex in which syx lacks the membrane anchor (residues 1–265); and the cytoplasmic domain of syx. Note that this form of SNAP25 is not palmitoylated, unlike that in vivo. The plasmids used to generate mouse synaptobrevin 2 (pTW2; (21)), the cytoplasmic domain of syb (pET-rVAMP2CD;(21)), the t-SNARE complex composed of rat syntaxin 1A and mouse SNAP25B (pTW34;(23)), full-length syntaxin 1A alone (pTrcHis), and the cytoplasmic domain of syx (residues 1–265, pTW12; (21)) were kindly provided by J. E. Rothman (Memorial Sloan-Kettering Cancer Center, New York, NY).

Syb, the binary t-SNARE complex, and full-length syx were expressed as described previously (21,23). Bacterial pellets were resuspended (~10 ml per liter of culture) in resuspension buffer (25 mM Hepes-KOH, pH 7.4, 400 mM KCl, 10 mM imidazole, and 5 mM β-mercaptoethanol) and incubated for 20 min on ice after addition of 0.5 mg/ml lysozyme. Protease inhibitors (1 μg/ml aprotinin, pepstatinin A and leupeptin; 1 mM phenylmethylsulfonyl fluoride) were then added and samples were sonicated in 35 ml batches on ice for 2 × 45 s (50% duty cycle). Triton X-100 was added to 2.1% (v/v) and incubated for 15 min with rotation before centrifugation of the cell lysate at 27,000 × *g* for 30 min in a JA-17 rotor (Beckman, Fullerton, CA). For syb purifications, the supernatant was additionally clarified by centrifugation at 35,000 rpm in a Ti45 rotor (Beckman) for 60 min. After the addition of DNase I and RNase (Sigma (St. Louis, MO), 10 μg/ml), the supernatant was then incubated for >2 h at 4°C with Ni-NTA agarose (Qiagen, Valencia, CA; 0.5 ml of a 50% slurry per liter of cell culture) equilibrated in resuspension buffer. Beads were washed extensively with resuspension buffer containing 1% Triton X-100 and then washed with OG wash buffer (25 mM Hepes-KOH [pH 7.4], 400 mM KCl, 50 mM imidazole, 10% glycerol, 5 mM β-mercaptoethanol, 1% octylglucoside). The slurry was loaded onto a column, washed with 5–10 column volumes of OG wash buffer, and step eluted with OG wash buffer containing 500 mM imidazole.

The cytoplasmic domain of syb and the soluble t-SNARE complex were purified as described above, but all detergents were omitted from the wash buffers. The purified proteins were dialyzed against 25 mM Hepes-KOH (pH 7.4), 100 mM KCl, 10% glycerol, and 1 mM DTT.

The v-SNARE and t-SNARE vesicles were reconstituted by rapid dilution and dialysis and subsequently purified by flotation in an Accudenz (Accurate Chemical, Westbury, NY) step gradient as described previously (21). Phospholipids were from Avanti Polar Lipids (Alabaster, AL). v-SNARE vesicles were reconstituted using a lipid mix composed of 84% 1-palmitoyl, 2-oleoyl phosphatidylcholine (POPC), 15% 1,2-dioleoyl phosphatidylserine (DOPS), and 1.0% 1% head-labeled *N*-(tetramethylrhodamine)-1,2-dihepta-decanoyl phosphatidylethanolamine (TMR-DHPE, Molecular Probes, Eugene, OR). t-SNARE vesicles were reconstituted in 85% POPC and 15% DOPS (mol/mol). The copy number of syb or binary t-SNARE complexes is varied by dilution into OG wash buffer with 500 mM imidazole before addition to the lipid film. The protein recovered in the purified vesicles was determined by an amido black protein assay. The final buffer was 25 mM Hepes-KOH (pH 7.4), 100 mM KCl. Our standard v-SNARE vesicles contain ~100 copies/vesicle (protein/lipid ratio 1:240). Synaptic vesicles in vivo are estimated to carry ~30 copies of syb (22,30). Our standard binary t-SNARE vesicles contain ~0.8 copies/vesicle; ~70–80% of the syb or t-SNARE complexes are oriented with their cytoplasmic domains facing outward. The fraction of t-SNAREs in the planar bilayer that face up into bulk solution was not determined, but this has been 50% in similar studies (27). Protein-free vesicles are reconstituted and purified as described for the SNARE-containing vesicles.

In one of the controls, the v-SNARE vesicles were treated with 0.4 μM of the botulinum neurotoxin BoNT B for 3.5 h at 37°C before addition above the t-SNARE bilayer. BoNT B cleaves most of the cytoplasmic domain of syb. The detailed protocol is published elsewhere (24).

Formation and characterization of t-SNARE bilayers

Supported lipid bilayers are formed by vesicle fusion on a clean, hydrophilic glass coverslip, a well established technique pioneered by Tamm and McConnell (31). Coverslips were cleaned by sonication in detergent for 1 h (CONTRAD 70, Decon Laboratories, King of Prussia, PA), thorough rinsing in Millipore water (Simplicity 185, Millipore, Billerica, MA), sonication in Millipore water for 30 min, and exhaustive rinsing in Millipore water. They were stored overnight at 90°C in Nano-Strip (Cyantek, Fremont, CA), a commercial mixture of H_2O_2 and concentrated H_2SO_4, and again rinsed thoroughly immediately before use. The bilayers ''float'' on a 1–2 nm layer of water and exhibit fast diffusion of lipids in both leaflets and of many peripheral membrane proteins (32,33). We studied a range of conditions for deposition of the t-SNARE bilayer by proteoliposome fusion on glass. The average number of t-SNAREs per liposome was either ~0.8 (''low t-SNARE-density bilayers'', similar to the Brunger-Chu study (27) or ~80 (''high t-SNARE-density bilayers''). The total lipid concentration was usually 25 μM, and deposition temperatures of 4°C, 25°C, and 37°C and times of 2–3 h were explored. After deposition, the bilayers were warmed to the desired temperature (either 25°C or 37°C) for 1 h and gently washed three times with buffer (60 cell volumes total) just before docking and fusion studies.

Wide-field fluorescence microscopy using 0.1% labeled lipids enabled assessment of the quality of the resulting t-SNARE bilayers on a 200 nm–20 μm scale. Bilayers formed directly at 37°C often exhibited dark, round defects of diameter ~1 μm, evidently due to regions of bare glass. The v-SNARE vesicles docked efficiently to these defects. Deposition at 25°C led to smooth bilayers, but gave docking and fusion behavior that depended on deposition time in the range of 2–3 h. Deposition at 4°C followed by warming to 25°C or 37°C and washing minimized defects and thus became the preferred procedure.

Fluid-phase, variable temperature, tapping mode atomic force microscopy (AFM) was used to assess the quality of bilayers on a 10 nm–1 μm scale formed under conditions quite similar to those in the optical docking and fusion assay (Fig. 1). We used force-modulation etched silicon probes (FESP tips, Veeco Metrology Group, Santa Barbara, CA) in a commercial instrument (NanoScope IV, Digital Instruments, Buffalo, NY). Samples were scanned at 2 Hz. Fusion of protein-free vesicles on glass leads to the expected relatively smooth surface with few defects. ''Plowing'' the bilayer surface to expose glass and rescanning the same region reveals the apparent height of the deposited material as 4.5 ± 0.7 nm, consistent with the expected height of a POPC/DOPS bilayer. The apparent surface roughness is similar to that of the underlying glass surface, root-mean-square (rms) ~0.3 nm. In contrast, t-SNARE bilayers deposited using a larger copy number of ~80 t-SNARE/liposome and 250 μM total lipid exhibit large ''mountains'' of aggregated protein/lipid material above the smooth bilayer terrace that withstand the raster scan of the AFM tip. These mountains are irregular in shape, with lateral dimensions on the order of tens of μm and height ~50 nm (not shown). Such surfaces were not studied further. Deposition using 80-copy t-SNARE vesicles at 10 times lower overall vesicle concentration (25 μM total lipid) leads to the smaller aggregates we call ''mounds'' (~0.4 μm laterally and ~10 nm taller than the bilayer itself (Fig. 1 *a*). We refer to these surfaces as the ''high t-SNARE-density'' bilayers. By direct count, the surface density of the mounds is 0.2 ± 0.1 μm^{-2}, remarkably consistent with the estimated density of v-SNARE vesicle binding sites on the same bilayers (T_0 = 0.1 μm^{-2}, below). After deposition with the preferred t-SNARE copy number of ~0.8 and 25 μM total lipid, AFM images (Fig. 2 *b*) look very similar to those of a protein-free surface. The rms roughness is again ~0.3 nm. There is no evidence of protein-related features, probably because the AFM tip pushes small t-SNARE monomers or clusters along the surface as it rasters. We refer to these surfaces as the ''low t-SNARE-density'' bilayers.

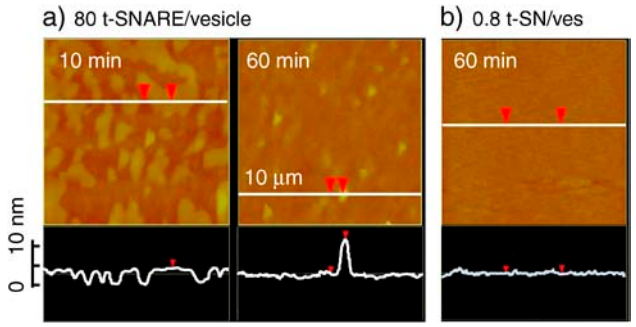

FIGURE 1 AFM images of t-SNARE bilayers. Tapping-mode AFM images of 10 μm × 10 μm patches of t-SNARE bilayer formed by deposition of vesicles on a hydrophilic glass substrate at T = 37°C. Relatively high regions are bright yellow, whereas relatively low regions are dark brown. Scans (10 μm) of apparent height along the white, horizontal lines are shown below each image (0–10 nm height scale at *left*). Red triangles are position markers not of interest here. (*a*) Deposited from vesicles with ~80 t-SNARE copies on average at total lipid concentration 25 μM. Image at left (10-min incubation) shows ridges of lipid bilayer (*yellow*) with nominal height 4.3 nm above bare glass (*brown*). Image at right (60-min incubation) shows large regions of flat bilayer (*brown*). The bright yellow spots are evidently ''mounds'' of t-SNARE material that rise 5–10 nm above the bilayer surface and have lateral dimensions of ~400 nm. (*b*) After 60-min incubation time with vesicles of ~0.8, t-SNARE copies on average at total lipid concentration 25 μM. No mounds appear. The root mean-square vertical displacement is 0.3 nm, comparable to that of bare glass.

Docking and fusion assay by fluorescence microscopy

A modified commercial wide-field microscope (Eclipse TE2000-U, Nikon, Melville, NY) enables excitation of fluorophores at the glass/water interface by ''through the objective'' total internal reflection (TIR) (34). A 0.1 mW, cw laser at 514 nm illuminates a ~200-nm thick, 50-μm diameter cylinder including the lipid bilayer. We use a 100×, numerical aperture = 1.45 oil-immersion objective (Olympus, Melville, NY). Fluorescence from TMR-DHPE passes a 565–595 nm bandpass filter (D580/30, Chroma, Rockingham, VT) and is imaged onto a fast charge-coupled device camera (I-Pentamax, Roper Scientific, Trenton, NJ), yielding digital movies of fluorescence intensity versus time. The camera pixels are square, 15 × 15 μm^2, corresponding to 150 × 150 nm^2 in real space at the sample. Most movies used a 250 × 250 pixel region of interest and 40-ms frames for periods of 2–10 s. For accurate measurement of the distribution of times to fusion t_{fus}, we restricted the region of interest to 150 × 98 pixels and used the ''virtual chip'' mode of the camera. This enables 5-ms or 10-ms frames that more accurately capture the time delay between firm docking and fusion.

The t-SNARE bilayer is formed on a glass coverslip that serves as the TIR window of the fluorescence microscope and also forms one wall of a small-volume flow cell. The cell volume is cylindrical, 1 mm tall × 8 mm diameter (50 μL). Quantitative measurement of docking kinetics requires a reproducible method for placing v-SNARE vesicle solution at a known bulk concentration in contact with the t-SNARE bilayer surface rapidly and uniformly. Using a pipette, we flow four times the cell volume of v-SNARE vesicle solution through the cell, fully exchanging solution in ~2 s. Docking/fusion movies begin 10–20 s later, after manually focusing the microscope. Docking traces up to 16 min long are acquired in time-lapse

mode, for which the laser illuminates the sample for 40 ms during each 2-s frame interval.

The mean fluorescence intensity of a docked but unfused vesicle is smaller than that of a docked and fused vesicle by a factor of 2–4, as described below. This requires a different procedure for measuring the surface density of unfused and fused vesicles. Fortunately, each experimental condition yielded essentially no fusion or essentially complete fusion of docked vesicles, so it was not necessary to blend the procedures. For docking without fusion, a centroid algorithm locates and counts vesicles in each frame using an intensity threshold. This direct count yields the total surface concentration of docked but unfused vesicles, $D(t)$ in the kinetics model of Eq. 2 below. When fast fusion dominates, the laser seldom illuminates a docked vesicle within the 2-s frames of a time-lapse movie (laser-on duty factor of only 0.02). Instead, most vesicles are imaged only as fusion products, which appear as dim, diffuse clouds. Therefore we measure the total fluorescence intensity versus time, $I_{tot}(t)$, and calibrate the mean intensity per fused vesicle using 2-s long movies acquired with 40 ms frames and low vesicle density, so that single docking and fusion events are captured faithfully. A correction for slow photobleaching was also applied. The resulting absolute number density of fused vesicles is accurate to $\pm 10\%$.

Enhancement of fluorescence intensity after fusion

We show below that fusion causes a sudden enhancement of a factor of 2–4 in the fluorescence intensity from the vesicle's labeled lipids. The fused vesicle's lipids lie entirely in the most intense part of the evanescent field. Before fusion, a 50-nm vesicle samples a modest range of intensities. However, this is a small effect because the 50-nm vesicle diameter is substantially smaller than the estimated $1/e$ penetration depth of the evanescent field into the bilayer/water layer of 150 nm. In separate experiments carried out on a bulk sample of identically labeled v-SNARE vesicles in a standard fluorimeter, we measured an enhancement of the entire fluorescence spectrum by a factor of 1.8 after complete solubilization of the lipids with detergent (data not shown). We attribute this to dequenching of TMR fluorescence, perhaps including dissociation of TMR dimers. Two polarization effects further enhance the postfusion intensity. The polarization of the TIR laser lies parallel to the plane of the bilayer (*s*-polarization), and both the absorption and emission transition dipole moments of TMR also preferentially orient parallel to the local bilayer plane (35). First, the TMR molecules are more efficiently excited by the laser after fusion, when all transition dipoles lie near the bilayer plane, than before fusion, when they are distributed randomly on the spherical surface of the vesicle. A geometric average of $\cos^2\theta$ (angle between the laser polarization axis and the transition dipole) over a random distribution of orientations on a sphere versus a disk shows that excitation could be enhanced by as much as a factor of 1.5. Second, the fluorescence collection efficiency also improves after fusion, because dipoles with horizontal polarization emit more of their intensity toward the objective than those with vertical polarization. The nearby glass surface also differentially affects fluorescence collection, further favoring postfusion emission (36,37). The combination of dequenching and the two polarization effects combine to explain the factor of 2–4 enhancement of intensity observed immediately after fusion.

RESULTS

Single-vesicle docking and fusion assay

This section describes the overall behavior of the assay, including evidence for full vesicle fusion and a qualitative discussion of various control experiments. Quantitative details of docking and fusion kinetics follow. We focus initially on the behavior of low t-SNARE-density bilayers (Materials and Methods) at 37°C. There is no Ca^{2+} or Mg^{2+} in these initial studies. The standard concentration of total lipid in the v-SNARE vesicle solution placed above the bilayer is 2.5 ± 0.8 μM, which translates to bulk vesicle concentration of $V_0 = (1.3 \pm 0.4) \times 10^{-10}$ M.

Direct observation of vesicle docking and full fusion

Docking and fusion of vesicles is described in Fig. 2. As an example of docking without fusion, Fig. 2 *a* shows a field of fluorescently labeled, protein-free vesicles at $t = 50$ s after their addition above the t-SNARE bilayer. Supplementary Movie 1 shows ''swarming'' behavior of protein-free vesicles that approach the surface and linger for several frames, but do not dock to form stable vesicle-planar bilayer complexes. The vesicles that do stick to the surface dock abruptly and subsequently move <70 nm rms. Repeated gentle washing with buffer does not remove any of the docked vesicles. Quantitative kinetics measurements show that compared with v-SNARE-containing vesicles, relatively few protein-free vesicles bind to low t-SNARE-density bilayers. For one such docked vesicle, Fig. 2 *d* shows the integrated fluorescence intensity within a circle of radius 0.7 μm centered at the docking position of one vesicle. We call this $I_{0.7\mu m}(t)$. On a 2-min timescale, we observe no evidence of either vesicle fusion or partial lipid mixing; the latter would lead to a gradual decrease in vesicle intensity and increase in background intensity over time. The distribution of fluorescence intensities of the protein-free vesicles of the species that bind to the bilayer is shown in Fig. 2 *e*. The long tail toward high intensity could be due to vesicle dimers, trimers, etc. as well as a broad distribution of single-vesicle sizes.

In sharp contrast, v-SNARE vesicles dock efficiently and fuse promptly on the same t-SNARE bilayers (Supplementary Movies 2 and 3). Fig. 2 *b* shows a snapshot of a t-SNARE bilayer the same 50 s after addition of a standard aliquot of v-SNARE vesicles. The high-intensity spots are the few remaining vesicles that have docked but not fused. The bright, hazy background is due to labeled lipids that have fused with the planar bilayer and undergone free lateral diffusion. It is clear by inspection that v-SNARE vesicles dock on the t-SNARE bilayer much more efficiently than protein-free vesicles. Movies 2 and 3 show that there is typically little or no motion away from the point of initial ''contact'' of the vesicle with the surface. Compared with protein-free vesicles, fewer ''swarming'' v-SNARE vesicles are observed.

For those vesicles that dock for at least one 40-ms camera frame before fusing, $I_{0.7\ \mu m}(t)$ shows a characteristic sharp increase in intensity by a factor of ~ 2 that persists for 1–2 frames (Fig. 2 *f*), followed by a monotonic, nonexponential decay on a timescale of ~ 1 s. With 5-ms frames, the intensity increase is a factor of 2–4 due to improved time resolution (see below). As seen in Movies 2 and 3 and in the sequence of images in Fig. 2 *c*, such events look like fast ''explosions''

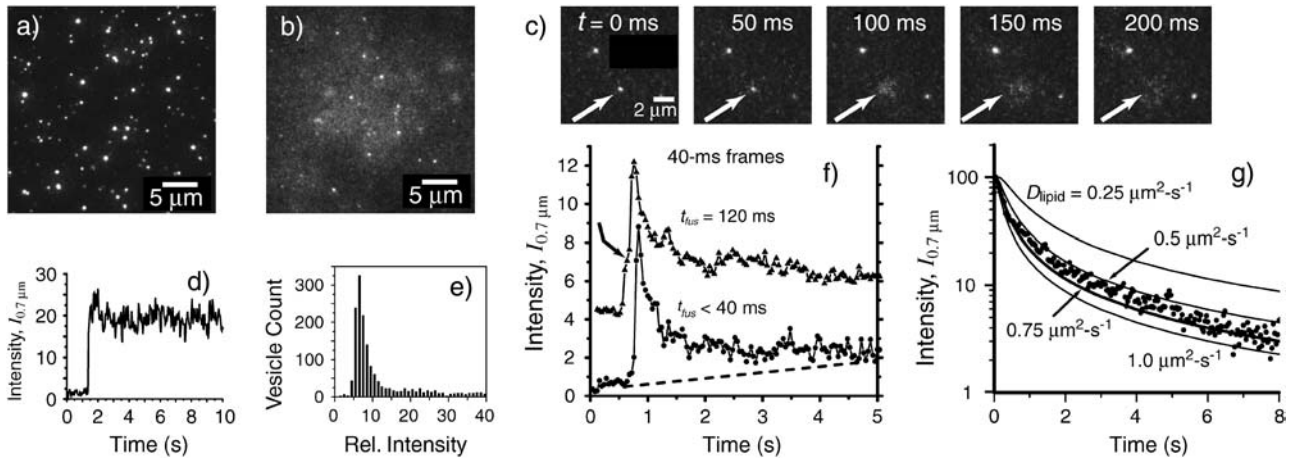

FIGURE 2 Fast fusion of v-SNARE vesicles on low t-SNARE-density bilayers. (*a*) Field of docked, protein-free vesicles 50 s after addition to a low t-SNARE-density bilayer. Sparse docking, but no fusion, has occurred. (*b*) Field of v-SNARE vesicles 50 s after addition to a low t-SNARE-density bilayer. The diffuse fluorescence is due to labeled lipids that have fused into the bilayer and dispersed. (*c*) Sequence of images spaced by 50 ms showing fusion of a v-SNARE vesicle and outward radial diffusion of the labeled lipids. (*d*) Relative integrated intensity in a circle of radius 0.7 μm, $I_{0.7\ \mu m}(t)$, for a docked but unfused vesicle (*frame a*) using 40-ms frames. (*e*) Histogram of relative integrated fluorescence intensities for docked, protein-free vesicles (*frame a*). (*f*) Two examples of $I_{0.7\ \mu m}$ (*t*) for vesicles that undergo fast fusion as in frame *b*. In the lower trace, fusion occurs within one camera frame of docking, followed by diffusion out of the circle on a ~1-s timescale. In the upper trace, the vesicle docks and waits three frames (marked by *arrow*) before fusion. Dashed line shows rising baseline due to leakage of labeled lipids from surrounding fusion events into the circle of integration. (*g*) Log plot of $I_{0.7\ \mu m}$ (*t*) for a single, well-isolated vesicle (no rising baseline). Lines are calculated by integrating Eq. 1 from $r = 0$ to 0.7 μm at each time *t* for various values of the diffusion coefficient D_{lipid} as shown. $D_{lipid} = 0.6 \pm 0.1\ \mu m^2\ s^{-1}$ best fits the data.

with good circular symmetry. The sharp rise in fluorescence intensity immediately after fusion is due to dequenching of the TMR labels and to polarization effects (Materials and Methods). Fusion of other vesicles nearby causes a slowly rising baseline on most traces.

The sharp rise in fluorescence occurs in one 5-ms camera frame or less. This sets an upper limit of ~5 ms on the timescale of lipid mixing. Evidently, the vast majority of events yield complete mixing of both vesicle leaflets with the planar bilayer. Fast hemifusion (mixing of the outer leaflet of the vesicle with the upper leaflet of the bilayer) would be readily observed as a partial ''explosion'' that leaves a bright core of ~40% of the original intensity behind. The core would be clearly visible if it persisted at least 0.3 s after hemifusion. In fact, only ~2% of the docked vesicles exhibit such behavior. These relatively rare events could be hemifusion, but they might also arise from docking of vesicle dimers or trimers (two or three v-SNARE vesicles bound together) and subsequent fusion of just one of the vesicles.

Fast diffusion of labeled lipids out of the observation circle makes the burst in $I_{0.7\ \mu m}(t)$ narrow in time. Assume that prompt, complete vesicle fusion instantaneously introduces a large, highly localized concentration of labeled lipids that subsequently diffuse radially outward in two dimensions with diffusion constant D. The time-dependent diffusion equation then predicts a Gaussian concentration profile that expands radially versus time (38):

$$C(r,t) = \frac{N*}{4\pi Dt}\exp(-r^2/4Dt). \quad (1)$$

Here, C has dimensions of molecules/μm^2 and $N*$ is the total number of labeled lipids released at $t = 0$. At each time, $C(r, t)$ peaks at $r = 0$; the radius at which $C(r, t)$ falls to half its peak value is $r_{1/2}(\mu m) = \sqrt{4\ln 2Dt} = 1.67\sqrt{Dt}$, with D in $\mu m^2\ s^{-1}$. In Fig. 2 *g*, we show a log plot of $I_{0.7\ \mu m}(t)$ for a single, high signal/noise, well-isolated fusion event with little baseline drift. The smooth curves are calculations of $I_{0.7\ \mu m}(t)$ obtained by integrating $C(r,t)$ from $r = 0$ to 0.7 μm at each time, with different values of D assumed. The calculation captures the nonexponential shape of the decay and mimics the data semiquantitatively for $D = 0.6\ \mu m^2\ s^{-1}$. This is comparable to lipid diffusion coefficients measured by single-lipid tracking of gold-labeled phosphatidylethanolamine in a supported egg PC/cholesterol bilayer at 25°C (0.3–0.7 $\mu m^2\ s^{-1}$. (39).

Because the vesicle's lipids promptly and completely dissolve in the bilayer in 5–10 ms or less, we infer that release of the vesicle's contents must occur at least that fast (''content-mixing'' in the vesicle-vesicle literature). The overall kinetics of fusion for the population of docked vesicles is a separate question addressed in detail below.

Requirement of v-SNAREs plus binary t-SNAREs or syntaxin alone

Control studies indicate that both docking and fusion are strongly enhanced by the simultaneous presence of v-SNAREs in the vesicles and binary t-SNAREs in the planar bilayer. The control results differ from the baseline data both in the

greatly reduced number density of effective vesicle binding sites and in the inability of the docked vesicles to fuse. The controls show that:

1. v-SNARE vesicles dock very little on protein-free bilayers and do not fuse.
2. Protein-free vesicles dock to a moderate extent on t-SNARE bilayers but do not fuse.
3. The docking of both protein-free vesicles and v-SNARE vesicles on t-SNARE bilayers is completely blocked by preincubation of the bilayer for 5 min with 5 μM of the cytoplasmic domain of syb (cd-VAMP). Presumably the cytoplasmic domain of syb binds efficiently to t-SNAREs to make *cis* SNARE complexes and prevent subsequent docking via *trans* SNAREs. The same effect evidently makes the surface less sticky toward protein-free vesicles.
4. The complementary control experiment preincubates the v-SNARE vesicles with cytoplasmic binary t-SNAREs (the cytoplasmic domain of syx complexed with SNAP25, 5 μM) for 5 min before addition to the t-SNARE planar bilayers. Again, docking is completely blocked.
5. Interestingly, we find that preincubation of the v-SNARE vesicles in 5 μM of cytoplasmic domain syx by itself also completely blocks docking of the vesicles to the t-SNARE bilayer. This suggests formation of a syb-syx complex that blocks full SNARE formation.
6. Bilayers formed from vesicles harboring $\sim$1 copy of full-length syx (without SNAP25) under otherwise identical conditions exhibit efficient docking and fast fusion of v-SNARE vesicles. The syx-only results are quantitatively indistinguishable from the binary t-SNARE results, as described below.

Effects of laser intensity, Ca^{2+} and Mg^{2+}, temperature, and t-SNARE density

Fusion in our system is fast in the absence or presence of dipositive cations. Preincubation of v-SNARE vesicles in 1 mM Ca^{2+} or Mg^{2+} changes the docking kinetics on low t-SNARE-density bilayers somewhat, but does not affect the fusion rate within experimental uncertainty. Quantitative details are given below. To test for possible thermal effects on fusion, we varied the laser intensity up and down by a factor of two, but observed no qualitative change in the fast fusion behavior. In addition, the degree of fusion observed on a particular bilayer is independent of the time delay between addition of the v-SNARE vesicles and the onset of laser illumination.

Docking and fusion are comparably efficient at 25°C and 37°C, although we carried out careful quantitative work only at 37°C. In several experiments, we deposited the low t-SNARE-density bilayer at 4°C for 2.5 h, warmed the bilayer to 25°C for 1 h, washed, and studied the docking and fusion at 25°C. As at 37°C, the v-SNARE vesicles dock efficiently and the vast majority fuse promptly at 25°C. However, after fusion, the labeled lipids often disperse into irregular, asymmetric patterns that suggest confinement in distinct lipid domains. The bilayer may segregate into domains at 4°C, with the t-SNAREs preferring one domain type over the other (40). Evidently the domains do not completely disperse in 1 h at 25°C, whereas the bilayer behaves homogeneously after 1 h at 37°C.

Finally, when the number of t-SNAREs per proteoliposome is increased from $\sim$0.8 to $\sim$80 to form the high t-SNARE-density bilayers (Materials and Methods), we observe much less efficient docking of v-SNARE vesicles and no fusion. These are the same surfaces that exhibit large mounds of t-SNARE protein in AFM images (Fig. 1 *a*). This strongly suggests that the t-SNAREs on the high protein density surface are somehow entangled and unable to form good *trans* SNARE complexes with syb. Addition of Ca^{2+} to the high t-SNARE density surfaces enhances the docking somewhat, but does not induce fusion on a 1-min timescale.

Quantitative docking kinetics

The simplest adsorption kinetics mechanism assumes that diffusion of solution-phase v-SNARE vesicles is sufficiently fast to maintain a concentration at the surface equal to the bulk v-SNARE vesicle concentration V_0. This is equivalent to the ''well-stirred reactor'' model described by the simple kinetics mechanism:

$$V(\text{solution}) + T(\text{surface}) \underset{k_{\text{undock}}}{\overset{k_{\text{dock}}}{\rightleftarrows}} D(\text{docked}) \overset{k_{\text{fus}}}{\rightarrow} F(\text{fusion}). \tag{2}$$

Here V represents the solution-phase v-SNARE vesicles; T represents the effective surface t-SNARE binding sites; D represents docked but unfused vesicles on the surface; k_{dock} and k_{undock} are adsorption and desorption rate constants; F represents fusion products on the surface; and k_{fus} is the unimolecular rate of fusion of docked vesicles. We use surface concentrations in vesicles-μm^{-2} and bulk concentrations in molar units, so k_{dock} has units $M^{-1}s^{-1}$, and k_{undock} and k_{fus} have units s^{-1}. The sum $D(t) + F(t)$ includes all vesicles that have docked up to time t, whether or not they have subsequently fused. The instantaneous total vesicle docking rate is the sum $R_{\text{dock}}(t) = dD/dt + dF/dt$ in vesicles $\mu m^{-2}\ s^{-1}$.

Under the assumptions that: 1), the bulk vesicle concentration $V = V_0$ is independent of time (many more vesicles than docking sites, which is true by design); 2), k_{undock} is effectively zero on the 16-min timescale of the experiments (as observed); and 3), diffusion rapidly fills the boundary layer just above the surface as adsorption occurs (which is only approximately true); the sum of docked and fused vesicles is a rising single exponential:

$$D(t) + F(t) = T_0[1 - \exp(-k_{\text{dock}}V_0t)]. \tag{3}$$

Here T_0 is the initial concentration of active surface sites and V_0 is the bulk vesicle concentration. Within the model, $D(t)$

$+ F(t)$ has initial slope $R_{dock}(t = 0) = k_{dock}T_0V_0$ and an asymptotic limit of T_0.

Examples of docking kinetics data are shown in Fig. 3. In Fig. 3 *b*, we show docking-plus-fusion kinetics plots for v-SNARE vesicles added to a bilayer formed with 0.8 t-SNARE/vesicle (the low t-SNARE-density bilayer) and to a bilayer formed with 80 t-SNARE/vesicle (the high t-SNARE-density bilayer). In both cases, the nominal concentration of total lipid was 2.5 ± 0.8 μM, which translates to bulk vesicle concentration of $V_0 = (1.3 \pm 0.4) \times 10^{-10}$ M, assuming 2.0×10^4 lipids/vesicle (outer leaflet of 50 nm diameter, inner leaflet of 40 nm diameter, 0.65 nm^2 per vesicle head). Clearly the initial docking rate R_{dock} and the effective total density of binding sites T_0 are at least 20 times larger for the low t-SNARE-density bilayer than for the high t-SNARE-density bilayer. Fig. 3 *c* shows examples of control measurements for protein-free vesicles docking to the low t-SNARE-density bilayer and for v-SNARE vesicles docking to the protein-free bilayer. Compared with v-SNARE vesicles on low t-SNARE-density bilayers (Fig. 3 *b*), T_0 is evidently ~10 times smaller for protein-free vesicles and ~100 times smaller for the protein-free bilayer. Quantitative fits will confirm these visual estimates. In several of these cases, the intrinsic docking rate constant will prove to be substantial; the primary effect of the controls is to drastically reduce the density of effective binding sites.

For v-SNARE vesicles docking to the low t-SNARE-density bilayer, a least-squares fit of the data to the equation

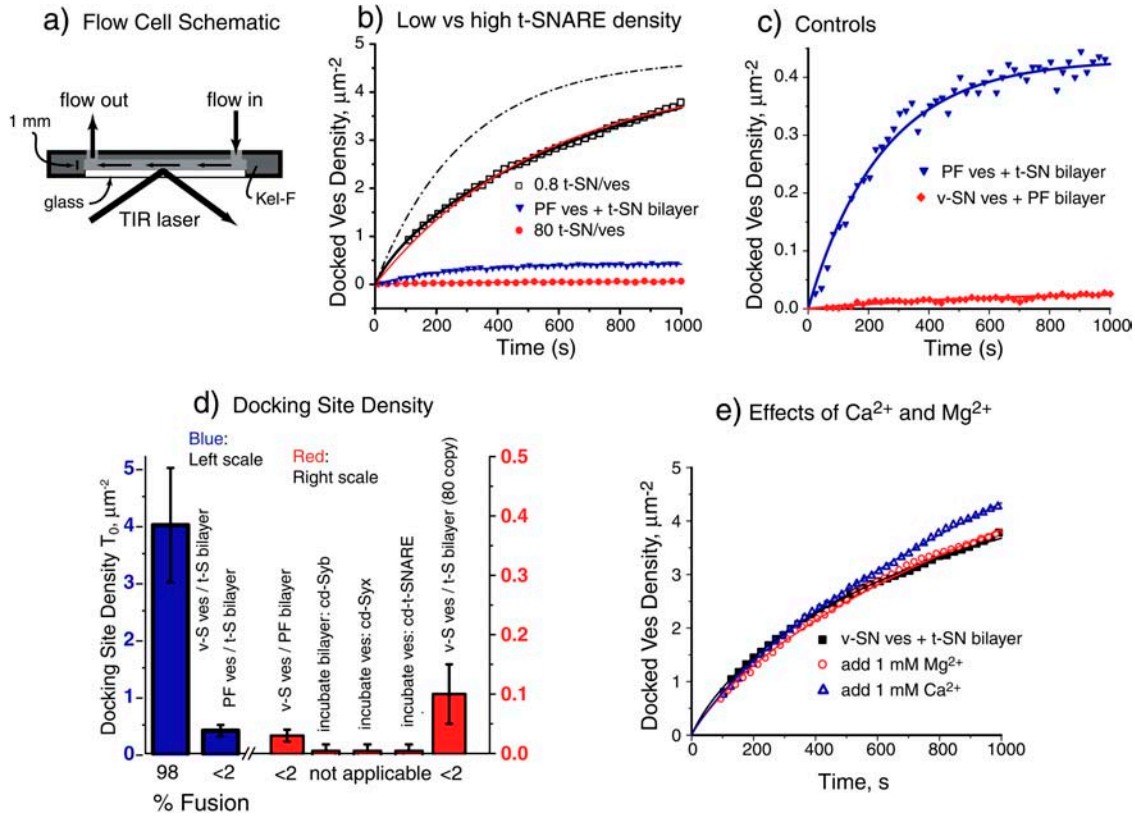

FIGURE 3 Docking kinetics. (*a*) Schematic of flow cell for vesicle docking kinetics experiments. (*b*) Plots of total surface density of docked vesicles versus time, whether fused or unfused (Materials and Methods). (□) v-SNARE vesicles on low t-SNARE-density bilayer. Red line is least-squares fit to simple adsorption model (Eq. 3), yielding $k_{dock} = 1.1 \times 10^7$ M^{-1} s^{-1} and adsorption site density $T_0 = 4.4$ μm^{-2}. Black line is hand-adjusted best fit to the diffusion-adsorption model (see text and Supplementary Material), with $k_{dock} = 2.0 \times 10^7$ M^{-1} s^{-1} and $T_0 = 4.7$ μm^{-2}. The values of $D_{ves} = 3.3$ μm^2 s^{-1} and $V_0 = 1.7 \times 10^{-10}$ M were held fixed. The dot-dash line shows the prediction of the simple kinetics model (Eq. 3) using the same values of k_{dock} and T_0. (*Red circles*) v-SNARE vesicles on high t-SNARE-density bilayer. Best-fit value is $T_0 = 0.10$ μm^{-2}, 40 times lower than the effective site density on the low t-SNARE-density bilayer. (*Blue triangles*) Protein-free vesicles on low t-SNARE-density bilayer. These data are repeated in frame *c* to emphasize the change of vertical scale. (*c*) Docking of v-SNARE vesicles on low t-SNARE-density bilayers as in frame *b* for two controls. Note vertical scale change from frame *b*. Lines are best fits to the diffusion-adsorption model. (*Blue inverted triangles*) Protein-free vesicles on low t-SNARE-density bilayer; $T_0 = 0.4$ μm^{-2}. (*Red circles*) v-SNARE vesicles on protein-free bilayer; $T_0 = 0.03$ μm^{-2}. (See Table 1 for all fitting results.) (*d*) Summary of absolute docking site density for v-SNARE vesicles on low t-SNARE-density bilayer (*leftmost bar*) and for all controls as indicated. Blue bars refer to left-hand scale, red bars to right-hand scale. ''v-SN ves'' means v-SNARE vesicle; ''t-SN'' means binary t-SNARE; ''PF'' means protein-free. Preincubations of the binary t-SNARE bilayer with cytoplasmic domain syb, and of the v-SNARE vesicles with the cytoplasmic domain of syx and with the cytoplasmic domain of the binary t-SNARE as shown. (*Below*) Percent of fusion-active vesicles, defined as the number of vesicles that fuse in 4 s divided by the total number of vesicles that dock in 4 s. (*e*) Docking curves for v-SNARE vesicle on low t-SNARE-density bilayers with addition of 1 mM Mg^{2+} and Ca^{2+}, compared with standard buffer as indicated.

$D(t) + F(t) = T_0\,[1 - \exp(-k_{expt}t)]$ is shown as the thin red line in Fig. 3 *b*. The best-fit values are $T_0 = 4.4\ \mu m^{-2}$ and $k_{expt} = 0.00182\ s^{-1}$, yielding $k_{dock} = k_{expt}/V_0 = 1.1 \times 10^7\ M^{-1}\ s^{-1}$ (with $V_0 = 1.7 \times 10^{-10}$ M as below). The reproducibility across different samples is $\sim\pm25\%$ in k_{dock} and $\pm40\%$ in T_0. The fit is reasonably good, but the simple model cannot accurately capture the detailed curvature of the data. This arises primarily from depletion of the vesicle concentration at the surface by adsorption, as shown below. In addition, the binding sites likely vary in t-SNARE cluster size and in the probability that a vesicle docks irreversibly when it touches a site. The resulting heterogeneity in k_{dock} could give rise to faster than average docking initially, as the more favorable sites would be filled first.

We further tested the model by doubling the bulk vesicle concentration to $2V_0$. The resulting data (not shown) could not be fit by the simple model with values of k_{dock} and T_0 at all comparable to the best-fit values derived from the data taken at V_0. This led us to investigate a more accurate ''diffusion-adsorption'' model that explicitly includes the effects of depletion of the concentration of v-SNARE vesicles at the surface. This standard ''unstirred reactor'' problem must be solved numerically with assumed input values of T_0, V_0, k_{dock}, and D_{ves}, the diffusion coefficient of v-SNARE vesicles in bulk buffer solution (41). The details are given in the Supplementary Material. In practice, we fixed $D_{ves} = 3.3\ \mu m^2\ s^{-1}$, as directly measured previously for comparable 50-nm diameter vesicles (42). We treated T_0 and k_{dock} as manually adjustable parameters and V_0 as a mildly adjustable parameter within its estimated $\pm30\%$ accuracy. Extensive exploration showed that the data can be very well fit, including the details of curvature, using the best estimate of $V_0 = 1.3 \times 10^{-10}$ M. However, other data sets, especially the docking of v-SNARE vesicles in the presence of Ca^{2+} and Mg^{2+}, were not well fit unless V_0 was adjusted mildly upward to 1.7×10^{-10} M. For consistency, we chose to fix V_0 at this latter value in all of the fitting, leaving only k_{dock} and T_0 as adjustable parameters.

As shown in Fig. 3 *b*, the diffusion-adsorption model fits the curvature of the kinetics plot significantly better than the simple model. In the example in Fig. 3 *b*, the best-fit values are $k_{dock} = 2.0 \times 10^7\ M^{-1}\ s^{-1}$ and $T_0 = 4.7\ \mu m^{-2}$. In conditions for which adsorption is efficient, like the v-SNARE plus t-SNARE data shown, the main effect of the diffusion-adsorption model compared with the simple model is to increase k_{dock} by a factor of ~2; T_0 remains essentially the same. As expected, the effect on k_{dock} is more modest for the controls with smaller T_0, since diffusion is then better able to keep up with adsorption. The need to include diffusion explicitly is underscored by the dot-dash curve in Fig. 3 *b*, which shows the prediction of the simple adsorption model using the best-fit kinetic parameters from the diffusion-adsorption model. The diffusion-adsorption model also shows clearly why the approach to the asymptote T_0 is so slow. According to the model, it would take 2000 s = 33 min for the surface density to reach 95% of its asymptote. In practice, we found that photobleaching and defocusing of the microscope limited our ability to obtain accurate data beyond $\sim$1000 s.

The ''best-fit'' diffusion-adsorption result in Fig. 3 *b* is not a least-squares fit, but rather the result of trial and error. The calculated adsorption curve is highly sensitive to the combination of input parameters. For fixed D_{ves}, the product $k_{dock}T_0$ controls the initial slope (as in the simple model); T_0 controls the long-time asymptote; and k_{dock} and V_0 affect the curvature of the approach to saturation of the surface sites. The most important derived parameters k_{dock} and T_0 separate reasonably well, but we are unable to set statistically valid error limits on the results. Our manual fitting procedure consistently locks on to very similar ''best-fit'' values for a given data set, and k_{dock} is reproducible across nominally identical samples to $\sim\pm25\%$. The best-fit T_0 varies by $\pm50\%$ across nominally identical samples. Much of the variability is probably due to real differences in the quality of the t-SNARE binding sites from sample to sample.

TABLE 1 Summary of docking and fusion kinetics parameters

Conditions*	k_{dock} ($M^{-1}\ s^{-1}$)†	T_0 (site μm^{-2}) †	k_{fus} (s^{-1})
v-SN ves on t-SN bilayer (0.8 copy)	$(2.2 \pm 0.4) \times 10^7$	4 ± 1	40 ± 15‡
Protein-free ves on t-SN bilayer (0.8 copy)	$(2.8 \pm 0.5) \times 10^7$	0.4 ± 0.1	<0.0002§
v-SN ves on protein-free bilayer	$(8 \pm 4) \times 10^6$	0.03 ± 0.01	<0.0002§
v-SN ves + 1 mM Mg^{2+} on t-SN bilayer (0.8 copy)	$(1.4 \pm 0.4) \times 10^7$	8 ± 1	>15¶
v-SN ves + 1 mM Ca^{2+} on t-SN bilayer (0.8 copy)	$(5 \pm 3) \times 10^6$	25 ± 10	>15¶
v-SN ves on t-SN bilayer (80 copy)	$(1.2 \pm 0.7) \times 10^7$	0.10 ± 0.05	<0.0002§

*t-SN bilayer (0.8 copy) and (80 copy) denote the low and high t-SNARE-density bilayers (Materials and Methods). See Fig. 1 for AFM images of these surfaces. Other abbreviations as in Fig. 3. Refer to Fig. 3 for additional control results.

†Results of least-squares fits to the diffusion-adsorption model (see text and Supplementary Material), with D_{ves} fixed at 3.3 $\mu m^2\ s^{-1}$ (42) and V_0 fixed at 1.7×10^{-10} M (see text). Each entry is the mean of 3–4 independent determinations on separate bilayers. Uncertainties span the range of results.

‡From fit of histogram of t_{fus} shown in Fig. 4 *b*.

§Conservative upper bound from the absence of vesicle fusion in 500 s movies.

¶Lower bound from histogram of t_{fus} with 40-ms bins; 5-ms movies were not taken with Ca^{2+} and Mg^{2+}.

Averages of the resulting model parameters from fits to the diffusion-adsorption model under various experimental conditions are collected in Table 1. Each entry is the mean of 3–4 independent determinations on separate bilayers. For v-SNARE vesicles docking to the low t-SNARE-density bilayer, we find $k_{dock} = (2.2 \pm 0.4) \times 10^7\ M^{-1}\ s^{-1}$ and an effective density of binding sites $T_0 = 4 \pm 1\ \mu m^{-2}$. Error estimates indicate the range of ''best-fit'' values across triplicate experiments. In contrast, the high t-SNARE-density bilayer shows efficient docking to a much smaller density of binding sites: $k_{dock} = (1.2 \pm 0.7) \times 10^7\ M^{-1}\ s^{-1}$ and $T_0 = 0.10 \pm 0.05\ \mu m^{-2}$. The low t-SNARE-density bilayer contains 100 times fewer t-SNAREs but evidently exhibits 40 times as many effective docking sites. We argue below that the binding sites on the high t-SNARE-density bilayer are the large domains of aggregated t-SNAREs directly observed by AFM (Fig. 1 *a*).

To test the effect on docking of removal of SNAP25 from the binary t-SNARE complex, we formed low syx-density bilayers in exactly the same way and added v-SNARE vesicles as before. Three bilayers of each type were directly compared on the same day. These resulting docking curves for low density binary t-SNARE bilayers and low density syx-only bilayers coincide within ±20% (data not shown). Inclusion of SNAP25 had no measurable effect on docking within our experimental reproducibility.

The quantitative analyses of the other controls reveal 10–40 times smaller effective binding site density T_0 (Fig. 3 *d* and Table 1). All of the intrinsic docking rate constants lie in the range 0.5×10^7–$2.8 \times 10^7\ M^{-1}\ s^{-1}$. Docking to the few available adsorption sites is fairly efficient in all the control experiments. All values of k_{dock} lie within a factor of 10 of theoretical estimates of the diffusion-limited docking rate constant to surface sites of effective radius $R \sim 7$ nm (Discussion). For very low T_0, surface imperfections may provide the bulk of the binding sites. However, the t-SNARE bilayers bind protein-free vesicles 10% as efficiently as they bind v-SNARE vesicles, suggesting a significant nonspecific interaction that cannot lead to fusion.

Fig. 3 *e* compares representative docking kinetics plots for v-SNARE vesicles on the low t-SNARE-density bilayer in plain buffer, in the presence of 1 mM Mg^{2+}, and in the presence of 1 mM Ca^{2+}. The solid lines are best fits to the diffusion-adsorption model. The three curves are qualitatively similar, but they differ substantially in their curvature. The plain buffer experiments rise more rapidly at early time. This effect requires additional study, but the diffusion-adsorption model consistently finds significantly lower values of k_{dock} and higher values of T_0 in the presence of Mg^{2+} or Ca^{2+} (Table 1). In future investigations, it will be important to improve the accuracy of V_0 and D_{ves} if subtle variations in k_{dock} and T_0 are to be interpreted with confidence.

In a final qualitative control, the v-SNARE vesicles were pretreated with BoNT B (as described in Materials and Methods), which acts by cleavage of the helix-forming cytoplasmic domain of syb. On the standard, low t-SNARE-density bilayer, docking of the pretreated vesicles is inhibited by a factor of three at all times relative to the untreated vesicles (data not shown). As judged by movies with 40-ms frames, those vesicles that dock proceed to fuse on a similar timescale to the normal v-SNARE vesicles, suggesting they have sufficient remaining intact syb to enable ternary SNARE-complex formation.

Quantitative fusion kinetics

In this section, we describe the fusion of v-SNARE vesicles on the low t-SNARE-density bilayer in quantitative detail. The single-vesicle assay enables measurement of the distribution of t_{fus}, the residence time of firmly docked vesicles on the surface before fusion. From the usual 40 ms/frame movies, which give good signal/noise ratio, we found that the time between docking and fusion is usually <80 ms, i.e., two frames or less (Fig. 2 *f*). This made it possible to set a lower limit $k_{fus} > 15\ s^{-1}$ but difficult to determine the actual decay rate. Using the fast camera mode enabled us to obtain docking and fusion movies at 10 ms/frame and 5 ms/frame (Supplementary Movie 3), albeit with low signal/noise ratio. Examples of traces of $I_{0.7\ \mu m}(t)$ from these fast movies (Fig. 4 *a*) usually show a distinct ''hesitation'' of 1–10 camera frames between docking and fusion, with fusion signaled by a sharp increase in intensity by a factor of 2–4 in one frame. We assign each fusion event to a 5-ms bin (bin 1: $0 < t_{fus} \le 5$ ms; bin 2: 5 ms $< t_{fus} \le 10$ ms; etc.). Both the $I_{0.7\ \mu m}(t)$ plot and visual inspection of each frame just before fusion are necessary for proper binning. The noisy intensity plot does not always distinguish a firmly docked vesicle from a vesicle that is ''searching'' the surface in the vicinity of its eventual docking site. However, the onset of the expansion of labeled lipids is often detected visually two frames later than the sharp jump in $I_{0.7\ \mu m}(t)$, due to the 150-nm equivalent size of the pixels and the optical resolution limit.

A histogram of 62 events with $t_{fus} < 100$ ms acquired in 10 movies using five different surfaces is shown in Fig. 4 *b*. This represents 77% of all the docking events observed during the 10-s movies. An additional 18 vesicles (23%) fused in the longer time range 0.1–4 s. For homogeneous fusion kinetics and sufficient camera speed, meaning that all vesicles and docking/fusion sites have the same k_{fus} and $\Delta t \ll k_{fus}^{-1}$, the histogram would peak in the first time bin and decay exponentially:

$$P(t_{fus}) = (1/N_0)[-dN(t_{fus})/dt_{fus}]\Delta t = k_{fus}\exp(-k_{fus}t_{fus})\Delta t. \quad (4)$$

Here $N(t_{fus})$ is the number of docked vesicles that have survived to time t_{fus}, N_0 is the total number of fusion events analyzed, $P(t_{fus})$ is the probability that a given vesicle fuses in the time bin centered at t_{fus}, and Δt is the bin width.

Even for $\Delta t = 5$ ms, many fusion events occur in two frames or less. The camera's time-averaging broadens the cusp of the exponential decay. A particular docking event may begin at any time within the first 5-ms camera frame. This significantly attenuates the probability that fusion is observed in the first camera frame, since many vesicles dock late in the frame. The lines in Fig. 4 *b* show simulations of this effect for different assumed values of k_{fus}, obtained by averaging Eq. 4 over a uniform distribution of docking times within the first camera frame. All simulations are normalized to 62 total events. The fast fusion events (those 77% of docked vesicles for which fusion occurs in 100 ms or less) are well modeled with $k_{fus} = 40 \pm 15\ s^{-1}$ ($\tau_{fus} = 25 \pm 15$ ms). The χ^2 statistic computed with Poisson-like weighting factors (variance of each nonzero channel estimated as the number of counts; each channel with no counts weighted as one) indicates that $k_{fus} = 40\ s^{-1}$ gives the best fit. The reduced χ-squared statistic $\chi^2_\nu = 0.64$, indicating the model is adequate. That is, we find no statistically significant heterogeneity in the population of fast-fusing vesicles or their docking sites. Values of $k_{fus} > 50\ s^{-1}$ place too many events at short times, whereas values of $k_{fus} < 30\ s^{-1}$ place too few events at short times and too many at long times. The 23% population of more slowly fusing vesicles (100 ms $< \tau_{fus} <$ 4 s) clearly indicates significant kinetic heterogeneity within the entire vesicle population or among their docking/fusion sites.

For protein-free vesicles docking to the low t-SNARE-density bilayers, we never observed a fusion event among 500 vesicles during time-lapse movies lasting 500 s. The conservative assumption of <10% fusion sets the upper limit $k_{fus} < 0.0002\ s^{-1}$, which we include in Table 1. Analogous limits are given for the other control conditions, none of which showed fusion on a comparable timescale to the v-SNARE vesicles on the low t-SNARE-density bilayer.

In several experiments, we preincubated the v-SNARE vesicles in 1 mM Ca^{2+} or Mg^{2+} before addition to the low t-SNARE-density bilayers. We obtained fusion movies only with the slower, 40-ms frames. The 40-ms histograms of t_{fus} look identical using normal buffer, on addition of 1 mM Ca^{2+}, and on addition of 1 mM Mg^{2+} (data not shown). This establishes the lower bounds $k_{fus} > 15\ s^{-1}$ in Table 1.

Finally, we tested for fusion on syx-only bilayers prepared in the same way as the low t-SNARE-density bilayers but without expressing SNAP25. The histogram of t_{fus} for 47 fusion events occurring in 100 ms or less after firm docking as observed in three separate movies with 5-ms frames is shown in Fig. 4 *c*. These represent ~80% of all the vesicles that docked on the syx-only surface. Clearly, the fusion is comparably efficient and comparably fast on the syx-only bilayers and the binary t-SNARE bilayers (Fig. 4 *b*). More data are needed to improve the statistics, test for heterogeneity, and determine k_{fus} accurately, so we do not include these results in Table 1. Both docking and fusion results are very similar with and without SNAP25.

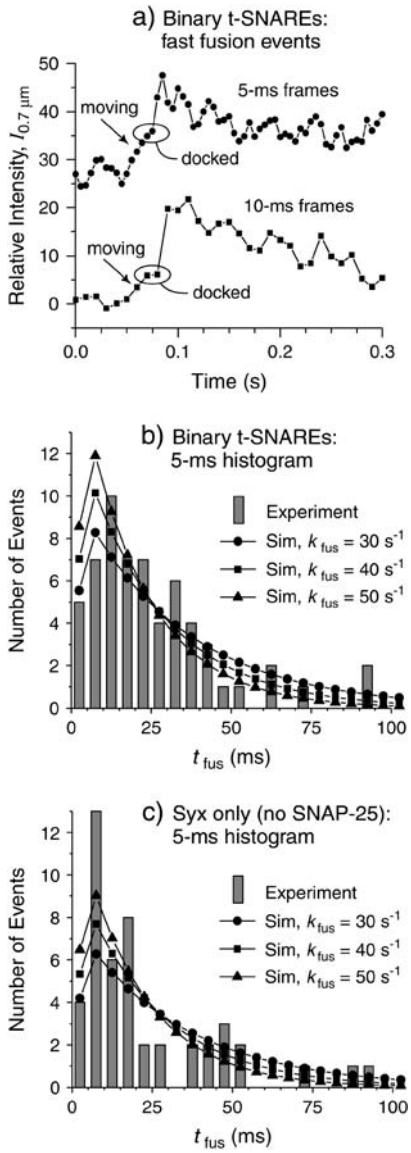

FIGURE 4 Fast fusion kinetics. (*a*) Examples of integrated intensity in a 0.7-μm radius circle, $I_{0.7\ \mu m}(t)$, for fast-fusing vesicles obtained with 5-ms and 10-ms camera frames on binary t-SNARE bilayers. The points within ovals are frames in which the vesicle was stationary (docked) before fusion. In the 5-ms trace, the three points preceding the oval correspond to frames in which the vesicle visits the circle of integration but is not yet firmly docked. See text for details. (*b*) Histogram of t_{fus} combining 62 events with $t_{fus} < 0.1$ s taken from 10 movies on five different binary t-SNARE bilayers. ''Sim'' traces show the results of averaging an exponential decay with k_{fus} as indicated over a uniform distribution of docking times relative to the camera frames, normalized to 62 total events. See text. (*c*) Histogram of t_{fus} combining 47 events with $t_{fus} < 0.1$ s taken from 11 movies on six different syx-only bilayers. ''Sim'' traces as in *b* but normalized to 47 total events.

DISCUSSION

Nature of fast fusion sites

The high absolute docking efficiency (see below), the absence of vesicle undocking, the preponderance of fast v-SNARE vesicle fusion events, and the success of the various control

experiments all strongly suggest that t-SNAREs within the active docking sites on the low t-SNARE-density bilayer interact freely and specifically with v-SNAREs to form ternary SNARE complexes that induce fast fusion. Quantitative modeling of the outgoing wave of labeled lipids (Fig. 2 *g*) shows that the sites also permit free release of the vesicle's lipids after fusion. However, the exact nature and stoichiometry of the docking/fast fusion sites is unknown. There is presumably a distribution of t-SNARE cluster numbers in the docking sites, potentially including monomers, dimers, and small multimers. The fusion assay finds remarkably little kinetic heterogeneity among the fast fusion sites.

The low t-SNARE-density bilayer is sparse in overall protein, with average lateral density ~100 t-SNARE/μm^2. This is 25 times larger than the estimated density of effective surface sites for v-SNARE binding ($T_0 = 4\ \mu m^{-2}$). Each binding site may be a t-SNARE multimer. In addition, some t-SNAREs may be inactive (e.g., lying face-down). In the movies at 5 ms/frame, v-SNARE vesicles are observed to ''search'' the surface briefly before docking firmly; they do not move perceptibly in the dwell time just before fusion. One possibility consistent with our observations is that most t-SNAREs are initially mobile monomers, but they diffuse and combine to form immobile clusters on the surface during the 3.5 h incubation/annealing time. Such immobile t-SNARE clusters are probably the primary docking and fast fusion sites. There is precedent for clustering of binary t-SNAREs in the literature (43). It is significant that the docked vesicles become immobile within 10–20 ms of first touching the surface. Especially in the 5-ms movies, we see evidence of a brief ''search'' of the local surface before firm docking. A vesicle docked to a freely mobile t-SNARE cluster would not seriously impede its diffusion. The diffusion coefficient of a 50-nm vesicle in buffer is 3.3 $\mu m^2\ s^{-1}$ (42), significantly larger than D_{lipid}. In future work, it is important to probe diffusion of the t-SNAREs and to better characterize the structure of the purported t-SNARE cluster sites using fluorescence resonance energy transfer, as demonstrated earlier (27,44,45).

Absolute docking efficiency

The ''intrinsic'' docking rate constant k_{dock} can be interpreted as the product of a diffusion-limited rate constant k_{diff} for vesicle docking site encounters and the probability of docking per encounter: $k_{dock} = k_{diff}\, p_{dock}$. We estimate k_{diff} from the theoretical expression for the diffusive flux that impinges on sparse, perfectly sticky, circular surface binding sites of radius R. The flux per binding site is given by: $k_{diff}V_0 = 4D_{ves}RV_0$ (vesicles/s), where V_0 is the concentration of v-SNARE vesicles and D_{ves} is the vesicle diffusion coefficient (38). We must assume a value for R, the effective radius of a docking site. The ~7-nm length of a SNARE complex is smaller than the ~25-nm radius of the vesicle. For the low t-SNARE-density bilayer, we take $R \sim 7$ nm to approximate the lateral reach of a single v-SNARE or t-SNARE (8). Inserting $D_{ves} = 3.3 \times 10^{-8}\ cm^2\ s^{-1}$ then yields $k_{diff} = 5.6 \times 10^7\ M^{-1}\ s^{-1}$, ~2.5 times the experimental value $k_{dock} = 2.2 \times 10^7\ M^{-1}\ s^{-1}$ (i.e., p_{dock} ~0.4). The t-SNARE sites on the low-density surface capture v-SNARE vesicles with high probability per encounter.

For v-SNARE vesicles adsorbing to the high t-SNARE-density bilayer, the primary docking sites are probably the large t-SNARE aggregates observed by AFM (Fig. 1 *a*). The relatively small density of effective docking sites on that bilayer ($T_0 = 0.1 \pm 0.05\ \mu m^{-2}$) is essentially the same as the density of aggregated t-SNARE mounds obtained by direct count on the AFM images ($0.2 \pm 0.1\ \mu m^{-2}$). Such sites are larger than the approaching vesicle, so we take R to be the ''radius'' of an aggregate: $R \sim 200$ nm. This gives $k_{diff} = 1.6 \times 10^9\ M^{-1}\ s^{-1}$, ~60 times larger than $k_{dock} = 1.2 \times 10^7\ M^{-1}\ s^{-1}$ (i.e., $p_{dock} \sim 0.02$). If the aggregates are indeed the binding sites, then the binding probability per encounter is very low. The t-SNAREs must be in very different condition on the low and high t-SNARE density surfaces.

Recent evidence suggests the possibility that binding of the SNARE-forming, cytoplasmic segment of syb to the vesicle bilayer itself provides one level of regulation of synaptic response. Electron paramagnetic resonance data indicate that insertion of the 7–8 residues nearest the membrane anchor inhibits formation of a ternary SNARE complex among anchored syb and the cytoplasmic domains of syx (lacking the H_{abc} domain) and SNAP25 (46). A protein-binding assay using reconstituted proteoliposomes, harvested chromaffin granules, or harvested synaptic vesicles reached the same conclusion (47,48). Our study provides direct evidence that ternary SNARE formation is reasonably efficient between anchored syb and anchored binary t-SNAREs that include the H_{abc} domain. Evidently anchored, binary t-SNAREs are better able than cytoplasmic domains to pry loose the anchor-proximal segment of syb and form full ternary SNARE complexes.

Comparison of in vitro fusion assays

The behavior of reconstituted fusion systems has varied widely across laboratories. A detailed comparison may help guide future improvements. In the vesicle-vesicle geometry, both bilayers are curved. The vesicle/planar-bilayer geometry more closely approximates that found in nature. All else being equal, we would expect a stronger driving force toward fusion (more negative ΔG) and thus a smaller barrier to fusion in the vesicle-vesicle assays than in the vesicle-planar bilayer assays. Yet the single-vesicle studies have consistently found substantially faster fusion.

Vesicle-vesicle assays

In the vesicle-vesicle assays, fusion is detected by fluorescence dequenching of labeled lipid components, with the

intensity calibrated in ''rounds of fusion''. Weber, Rothman, and co-workers first demonstrated SNARE-dependent fusion; in the optimized system, the time to the first round of fusion was ~20 min (20,21). Fusion was not regulated by Ca^{2+}, even in the presence of syt. Subsequent studies have all found slow fusion on a timescale of tens of minutes (22,42). Tucker, Weber, and Chapman demonstrated a fourfold enhancement of the fusion rate in the presence of Ca^{2+} and the cytoplasmic domain of syt, but fusion remained slow (24).

We can use our measured values of k_{dock} to estimate the time to one round of fusion in a hypothetical vesicle-vesicle assay whose proteins' docking behavior mimicked ours. In three-dimensional solution, the diffusion-limited reaction rate constant for vesicle-vesicle collisions is $k_{diff} = 4\pi N_0 (R_A + R_B)(D_A + D_B)$, where N_0 is Avogadro's number, A and B label the two types of vesicles, $R_A = R_B$ is the common vesicle radius, and $D_A = D_B$ is the common vesicle diffusion constant. If we take $R_A = R_B = 25$ nm and $D_A = D_B = 3.3 \times 10^{-8}$ cm^2 s^{-1} from the literature (42), then $k_{diff} = 2.5 \times 10^9$ M^{-1} s^{-1}. Typical bulk fusion assays use vesicle concentrations $C_{v\text{-}SNARE} \sim 12$ nM $\ll C_{t\text{-}SNARE} \sim 110$ nM. Under these pseudo-first-order conditions, a diffusion-limited fusion reaction (diffusion-limited docking followed by prompt fusion) would initially show exponential decay of the unfused v-SNARE vesicle population with pseudo-first-order rate constant $k_{eff} = k_{diff}\, C_{t\text{-}SNARE} \sim 280$ s^{-1} ($\tau_{eff} \sim 4$ ms). One full round of fusion would occur on a timescale of $\sim 2\tau_{eff} \sim 8$ ms. If $p_{dock} = 0.4$, as estimated for our low t-SNARE-density planar bilayer, the timescale for the first round of fusion lengthens to ~20 ms. If the t-SNAREs on the vesicles were aggregated and relatively inert like the mounds on the high t-SNARE-density bilayer, $p_{dock} = 0.02$ predicts ~0.4 s to the first round of fusion.

In fact, the observed time to one round of fusion is 20–50 min, ~5000 times slower than the longer of these estimates. For the fusion rate to be controlled by inefficient docking, the docking probability per encounter would have to be $\sim 10^{-5}$, much smaller than anything directly observed in our assay. Therefore, we strongly suspect that the fusion step itself is the bottleneck. Jahn and co-workers reached a similar conclusion (42). If so, then the time to the first round of fusion provides the rough estimate $k_{fus} \sim 0.001$ s^{-1}. This is $\sim 10^4$ times slower than in our vesicle-bilayer assay using the fusion-efficient low t-SNARE-density bilayer. It is consistent with the estimated upper bound $k_{fus} < 0.002$ s^{-1} for fusion of v-SNARE vesicles on the high t-SNARE-density bilayer in our work.

Significantly, our vesicle-planar bilayer assay uses the same materials and procedures as the Tucker-Chapman assay to make both the v-SNARE and t-SNARE vesicles. Evidently, the t-SNARE vesicles are the impediment to faster fusion in the vesicle-vesicle assay. We tentatively conclude that all vesicle-vesicle assays to date are fusion-rate limited. The high barrier to fusion may well arise from the entangled or aggregated state of the t-SNARE complexes on the vesicle surface, although we lack direct evidence of this. If our 80-copy t-SNARE vesicles contain ''preaggregated'' t-SNAREs, deposition of these vesicles might nucleate formation of large aggregated mounds on the glass substrate. In contrast, for average copy number ~0.8 t-SNARE/vesicle, such ''preaggregation'' is essentially impossible. The resulting low t-SNARE-density bilayers induce fast fusion of v-SNARE vesicles.

Vesicle-planar bilayer assays

The three single-vesicle studies themselves exhibit a wide range of behavior. The Simon study (28) found docking but little or no fusion in the absence of dipositive cations. Only 0.35% of the docked vesicles fused in 50 s. This corresponds to $k_{fus} \sim 7 \times 10^{-5}$ s^{-1}. (This is our calculation, aimed at placing all studies approximately on the same quantitative scale.) Either Ca^{2+} (or Mg^{2+}) induced fusion of 15% (or 4%) of the docked vesicles within 50 s. Half of these ''competent'' vesicles fused within 10 s of Ca^{2+} addition ($k_{fus} \sim 0.07$ s^{-1}). On removal of the regulatory H_{abc} domain of syx and without Ca^{2+}, 10% of docked vesicles fused in 50 s, and 70% of the competent vesicles fused within 20 s of docking ($k_{fus} \sim 0.06$ s^{-1}). Evidently, Ca^{2+} and Mg^{2+} enhance both the number density of fusion-active sites and k_{fus} itself, whereas removal of H_{abc} primarily increases the number density of fusion-active sites. The presence of H_{abc} endows each t-SNARE with two spatially separate helical bundles, which we suggest can ''cross-link'' pairs of t-SNAREs and thus enhance t-SNARE aggregation.

One significant difference between our work and the Simon study may be the density of t-SNAREs in the planar bilayer. They used average copy number ~8 t-SNARE/vesicle (lipid/protein 3000:1), 10 times smaller than the ~80-copy vesicles we used to form the *high* t-SNARE-density bilayers that exhibit large mounds of aggregated protein (Fig. 1 *a*). Both resulting bilayers exhibit very low fusion rates. We did not observe the triggering of fusion on addition of Ca^{2+} or Mg^{2+} observed earlier, perhaps suggesting that the t-SNARE bilayers in the Simon study are less entangled than in our 80-copy bilayers. It may also be significant that in the Simon study the t-SNAREs were reconstituted into 100% POPC vesicles.

Our low t-SNARE-density conditions have protein content quite similar to that in the Brunger-Chu study (27). They formed a low syx-density planar bilayer (0.1–100 syx/μm^2) by vesicle deposition using 100% eggPC (no PS) and subsequently added SNAP25 to form binary t-SNARE complexes in situ. The experimental conditions would prevent observation of prompt fusion events in the dark. Under laser illumination, ~50% of the vesicles fuse on a 10–20 s timescale at 37°C ($k_{fus} \sim 0.07$ s^{-1}, comparable to the Simon study with added Ca^{2+} or Mg^{2+}). Evidently the fusion is thermally activated by laser heating. Individual fusion events were

abrupt (sub-100 ms). At relatively high syx concentration (270 μm^{-2}, ~3 times higher than our low-density conditions), the mean number of SNARE complexes per docked vesicle was ~12, consistent with the suggestion that our fast fusion sites are t-SNARE clusters. As few as 1–2 SNAREs were sufficient to cause docking and thermally induced fusion. There was no Ca^{2+} effect.

The obvious differences between our work and the Brunger-Chu study lie in the lipid composition (synthetic 85% POPC/15% DOPS for us, 100% eggPC for them) and in the method of formation of anchored t-SNARE complexes. Our t-SNAREs are fully formed in vivo and harvested as a single entity, whereas Brunger-Chu added SNAP25 to syx preanchored in the planar bilayer. Although the fusion rate constants are very different in the two studies, in both cases the rate is remarkably insensitive to replacement of the binary t-SNARE by syntaxin alone, i.e., to the presence or absence of SNAP25. Equally remarkably, the measured docking kinetics in our study are indistinguishable with or without SNAP25.

All four helices in the full SNARE bundle are amphipathic, with hydrophobic sides facing inward in the bundle (8). This may explain why anchored syb is able to bind to anchored syx in both studies, and why preincubation of the v-SNARE vesicles in cytoplasmic-domain syx completely blocks docking to t-SNARE bilayers in our study. Such ''imperfect SNAREs'' might comprise various combinations of four helices (e.g., two from syx, none from SNAP25, and two from syb), only three helices, etc. Evidently, such imperfect SNAREs are able to form stable complexes and to drive fusion. There is some precedent for this idea in a recent study (49) demonstrating that large dense-core neurosecretory granules isolated from the bovine neurohypophysis spontaneously fuse with a planar lipid bilayer containing syntaxin 1A but no SNAP25.

Why are the docking and fusion rates indistinguishable in our assay with or without SNAP25, whereas in the recent vesicle-vesicle fusion assay truncations of SNAP25 that mimic the actions of BoNT A and E suppressed fusion? We already argued that because our assay and the Tucker-Chapman assay use the same v-SNARE vesicles, the bottleneck causing ~10-min fusion in the vesicle-vesicle assay must be due to the entangled condition of the t-SNAREs. Truncation of SNAP25 might somehow enhance the entanglement of the t-SNARE binding sites, rendering them more inert. In our assay, the 25-ms fusion remains slow on the molecular timescale, i.e., there is still a bottleneck to our fusion process as well. The results suggest that our bottleneck (and that in the Brunger-Chu assay) arises from the condition of the v-SNAREs or from the dynamics of *trans* SNARE formation after the v-SNARE vesicle has docked, not from the condition of the t-SNAREs. This may be related to the observation that insertion into the *cis* bilayer of the 7–8 residues of syb nearest the membrane anchor inhibits formation of a ternary SNARE complex among anchored syb and the cytoplasmic domains of syx and SNAP25 (45–47). Future experimental work will shed more light on this issue.

CONCLUSIONS AND PROGNOSIS

In summary, we have demonstrated how to use the single-vesicle methodology to independently measure v-SNARE vesicle docking and fusion rate constants on planar t-SNARE bilayers. Both rates are informative. On low t-SNARE-density bilayers, v-SNARE vesicles dock with ~40% efficiency per encounter with a binding site; ~77% of the docked vesicles achieve fast fusion with $k_{fus} = 40 \pm 15\ s^{-1}$ in the absence of Ca^{2+} and of syt. Complete lipid mixing (and thus content release) occurs within 5–10 ms. The fusion rate constant is ~1000 times faster than observed in previous single-vesicle assays and $\sim 10^4$ times faster than the combined docking/fusion rate observed in vesicle-vesicle assays. Our results indicate that the condition of the binary t-SNAREs on a vesicle or bilayer surface controls both the effective surface binding site density and also k_{fus}.

The role of SNARE complexes in presynaptic vesicle fusion remains controversial. Indeed, some workers (50) have raised legitimate questions as to whether the early vesicle-vesicle fusion assays (21) carried out at high protein/lipid ratio ~1:20 truly prove that ternary SNAREs are fusagens. Our new data demonstrate that *trans* SNARE complexes can drive fusion of v-SNARE vesicles having protein/lipid ratio of ~1:240 on a timescale of 25 ms at 37°C. The vesicle-planar bilayer geometry has more realistic curvature than the vesicle-vesicle geometry, and fast fusion occurs with or without Ca^{2+} and in the absence of all auxiliary proteins. We have not yet fully optimized the protein concentrations, method of deposition, lipid mixtures, or vesicle size in our assay. Measurement of the intrinsic free energy barrier to vesicle-plus-bilayer fusion for the optimal number of well-formed *trans* SNARE complexes now becomes an important goal. It will be technically feasible to measure fusion rate constants of 500 s^{-1} or faster using higher laser intensity and the new generation of charge-coupled device cameras.

Clearly SNARE complexes alone can drive vesicle fusion much more rapidly than previously observed. Is the current value $k_{fus} = 40\ s^{-1}$ sufficiently fast to explain the submillisecond synaptic response time of specific systems to the Ca^{2+} trigger event in vivo? Seemingly not. It is important to distinguish the time to the first presynaptic response (release of the first few vesicles) and the kinetic response time of the entire population of ''readily releasable'' vesicles (51). The presynaptic response time $\tau_{synapse}$ depends on the number of readily releasable vesicles N and the kinetic time constant $\tau_{fus} = k_{fus}^{-1}$ as $\tau_{synapse} \sim \tau_{fus}/N$. In goldfish bipolar neurons (52), the population of readily releasable vesicles is ~2000 per neuron and $\tau_{fus} \sim 120$ ms, so the presynaptic response time can be submillisecond. In contrast, in calyx of Held nerve terminals, the entire population of ~4000 readily releasable vesicles exocytoses with $\tau_{fus} \sim 0.6$ ms at 40 μM

Ca^{2+} (29). The corresponding $k_{fus} \sim 1700\ s^{-1}$ is ~40 times faster than our $k_{fus} = 40\ s^{-1}$.

It remains to be seen just how fast an optimized *trans* SNARE system alone can drive fusion. We currently have no information about the nature of the bottleneck in our system. The starting point for our measurement of t_{fus} is the time at which the vesicle firmly docks, i.e., when perceptible lateral motion ceases on a ~70 nm length scale. We do not know what the SNARE components are doing in the time between firm docking and fusion. Suppose one ternary SNARE can cause firm docking, but multiple SNAREs must form before fusion. In that case, k_{fus} may measure the time for complementary proteins on the *trans* bilayers to find each other. Alternatively, a sufficient number of ternary SNAREs may form very quickly and contents may release rapidly, but our assay is limited in response time by an activation barrier to lipid mixing that must be overcome by thermal energy. In comparison with our docking-fusion study, the starting configuration in synaptic vesicle exocytosis just upstream of the Ca^{2+} trigger is presumably highly specific. For example, preoriented and prefolded SNARE helices may be poised to assemble the ternary SNARE. Alternatively, a partially formed ternary SNARE complex may be poised to zipper rapidly. In future work, simultaneous study of contents release and lipid mixing combined with fluorescence resonance energy transfer studies of interprotein distances versus time will begin to elucidate the slow steps of SNARE-induced fusion in vitro. Addition of auxiliary proteins such as Ca^{2+}/syt and complexin may further enhance k_{fus}.

SUPPLEMENTARY MATERIAL

An online supplement to this article can be found by visiting BJ Online at http://www.biophysj.org.

J.C.W. thanks the National Science Foundation (CHE-0071458 and CHE-0452375), the University of Wisconsin Alumni Research Foundation, and the University of Wisconsin-Madison Department of Chemistry for support of this research. This study was further supported by grants to E.R.C. from the National Institutes of Health (NIGMS GM 56827 and NIMH MH61876) and the American Heart Association (0440168N). W.C.T. thanks the National Institutes of Health for a postgraduate fellowship. We thank Dr. Min Dong for materials and help with the BoNT B treatment of v-SNARE vesicles.

REFERENCES

1. Katz, B. 1969. The Release of Neural Transmitter Substances. Charles C. Thomas, Springfield, IL.
2. Augustine, G. J. 2001. How does calcium trigger neurotransmitter release? *Curr. Opin. Neurobiol.* 11:320–326.
3. Sollner, T. H. 2003. Regulated exocytosis and SNARE function (Review). *Mol. Membr. Biol.* 20:209–220.
4. Llinas, R., I. Z. Steinberg, and K. Walton. 1981. Relationship between presynaptic calcium current and postsynaptic potential in squid giant synapse. *Biophys. J.* 33:323–351.
5. Bai, J., and E. R. Chapman. 2004. The C2 domains of synaptotagmin—partners in exocytosis. *Trends Biochem. Sci.* 29:143–151.
6. Whiteheart, S. W., and E. A. Matveeva. 2004. Multiple binding proteins suggest diverse functions for the *N*-ethylmaleimide sensitive factor. *J. Struct. Biol.* 146:32–43.
7. Sollner, T., M. K. Bennett, S. W. Whiteheart, R. H. Scheller, and J. E. Rothman. 1993. A protein assembly-disassembly pathway in-vitro that may correspond to sequential steps of synaptic vesicle docking, activation, and fusion. *Cell.* 75:409–418.
8. Sutton, R. B., D. Fasshauer, R. Jahn, and A. T. Brunger. 1998. Crystal structure of a SNARE complex involved in synaptic exocytosis at 2.4 Å resolution. *Nature.* 395:347–353.
9. Chen, X., D. R. Tomchick, E. Kovrigin, D. Arac, M. Machius, T. C. Sudhof, and J. Rizo. 2002. Three-dimensional structure of the complexin/SNARE complex. *Neuron.* 33:397–409.
10. Hazzard, J., T. C. Sudhof, and J. Rizo. 1999. NMR analysis of the structure of synaptobrevin and of its interaction with syntaxin. *J. Biomol. NMR.* 14:203–207.
11. Matthew, W. D., L. Tsavaler, and L. F. Reichardt. 1981. Identification of a synaptic vesicle-specific membrane protein with a wide distribution in neuronal and neurosecretory tissue. *J. Cell Biol.* 91:257–269.
12. Perin, M. S., N. Brose, R. Jahn, and T. C. Sudhof. 1991. Domain structure of synaptotagmin (p65). *J. Biol. Chem.* 266:623–629.
13. Brose, N., A. G. Petrenko, T. C. Sudhof, and R. Jahn. 1992. Synaptotagmin: a calcium sensor on the synaptic vesicle surface. *Science.* 256:1021–1025.
14. Chapman, E. R. 2002. Synaptotagmin: a Ca^{2+} sensor that triggers exocytosis? *Nat. Rev. Mol. Cell Biol.* 3:498–508.
15. Tucker, W. C., and E. R. Chapman. 2002. Role of synaptotagmin in Ca^{2+}-triggered exocytosis. *Biochem. J.* 366:1–13.
16. Haque, M. E., and B. R. Lentz. 2004. Roles of curvature and hydrophobic interstice energy in fusion: studies of lipid perturbant effects. *Biochemistry.* 43:3507–3517.
17. Malinin, V. S., and B. R. Lentz. 2004. Energetics of vesicle fusion intermediates: comparison of calculations with observed effects of osmotic and curvature stresses. *Biophys. J.* 86:2951–2964.
18. Li, Y., X. Han, and L. K. Tamm. 2003. Thermodynamics of fusion peptide-membrane interactions. *Biochemistry.* 42:7245–7251.
19. Han, X., C. T. Wang, J. Bai, E. R. Chapman, and M. B. Jackson. 2004. Transmembrane segments of syntaxin line the fusion pore of Ca^{2+}-triggered exocytosis. *Science.* 304:289–292.
20. Nickel, W., T. Weber, J. A. McNew, F. Parlati, T. H. Sollner, and J. E. Rothman. 1999. Content mixing and membrane integrity during membrane fusion driven by pairing of isolated v-SNAREs and t-SNAREs. *Proc. Natl. Acad. Sci. USA.* 96:12571–12576.
21. Weber, T., B. V. Zemelman, J. A. McNew, B. Westermann, M. Gmachl, F. Parlati, T. H. Sollner, and J. E. Rothman. 1998. SNAREpins: minimal machinery for membrane fusion. *Cell.* 92:759–772.
22. Mahal, L. K., S. M. Sequeira, J. M. Gureasko, and T. H. Sollner. 2002. Calcium-independent stimulation of membrane fusion and SNAREpin formation by synaptotagmin I. *J. Cell Biol.* 158:273–282.
23. Parlati, F., T. Weber, J. A. McNew, B. Westermann, T. H. Sollner, and J. E. Rothman. 1999. Rapid and efficient fusion of phospholipid vesicles by the alpha-helical core of a SNARE complex in the absence of an N-terminal regulatory domain. *Proc. Natl. Acad. Sci. USA.* 96: 12565–12570.
24. Tucker, W. C., T. Weber, and E. R. Chapman. 2004. Reconstitution of Ca^{2+}-regulated membrane fusion by synaptotagmin and SNAREs. *Science.* 304:435–438.
25. Coppola, T., S. Magnin-Luthi, V. Perret-Menoud, S. Gattesco, G. Schiavo, and R. Regazzi. 2001. Direct interaction of the Rab3 effector RIM with Ca^{2+} channels, SNAP-25, and synaptotagmin. *J. Biol. Chem.* 276:32756–32762.
26. Peters, C., M. J. Bayer, S. Buhler, J. S. Andersen, M. Mann, and A. Mayer. 2001. Trans-complex formation by proteolipid channels in the terminal phase of membrane fusion. *Nature.* 409:581–588.
27. Bowen, M. E., K. Weninger, A. T. Brunger, and S. Chu. 2004. Single molecule observation of liposome-bilayer fusion thermally induced by

soluble *N*-ethyl maleimide sensitive-factor attachment protein receptors (SNAREs). *Biophys. J.* 87:3569–3584.

28. Fix, M., T. J. Melia, J. K. Jaiswal, J. Z. Rappoport, D. You, T. H. Sollner, J. E. Rothman, and S. M. Simon. 2004. Imaging single membrane fusion events mediated by SNARE proteins. *Proc. Natl. Acad. Sci. USA.* 101:7311–7316.
29. Wolfel, M., and R. Schneggenburger. 2003. Presynaptic capacitance measurements and Ca^{2+} uncaging reveal submillisecond exocytosis kinetics and characterize the Ca^{2+} sensitivity of vesicle pool depletion at a fast CNS synapse. *J. Neurosci.* 23:7059–7068.
30. Jahn, R., and T. C. Sudhof. 1994. Synaptic vesicles and exocytosis. *Annu. Rev. Neurosci.* 17:219–246.
31. Tamm, L. K., and H. M. McConnell. 1985. Supported phospholipid bilayers. *Biophys. J.* 47:105–113.
32. Johnson, S. J., T. M. Bayerl, D. C. McDermott, G. W. Adam, A. R. Rennie, R. K. Thomas, and E. Sackmann. 1991. Structure of an adsorbed dimyristoylphosphatidylcholine bilayer measured with specular reflection of neutrons. *Biophys. J.* 59:289–294.
33. Kiessling, V., and L. K. Tamm. 2003. Measuring distances in supported bilayers by fluorescence interference-contrast microscopy: polymer supports and SNARE proteins. *Biophys. J.* 84:408–418.
34. Axelrod, D. 2001. Selective imaging of surface fluorescence with very high aperture microscope objectives. *J. Biomed. Opt.* 6:6–13.
35. Harms, G. S., M. Sonnleitner, G. J. Schutz, H. J. Gruber, and T. Schmidt. 1999. Single-molecule anisotropy imaging. *Biophys. J.* 77: 2864–2870.
36. Thompson, N. L., K. H. Pearce, and H. V. Hsieh. 1993. Total internal reflection fluorescence microscopy: application to substrate-supported planar membranes. *Eur. Biophys. J.* 22:367–378.
37. Abney, J. R., B. A. Scalettar, and N. L. Thompson. 1992. Evanescent interference patterns for fluorescence microscopy. *Biophys. J.* 61: 542–552.
38. Berg, H. C. 1993. Random Walks in Biology. Princeton, N.J.: Princeton University Press.
39. Lee, G. M., A. Ishihara, and K. A. Jacobson. 1991. Direct observation of Brownian motion of lipids in a membrane. *Proc. Natl. Acad. Sci. USA.* 88:6274–6278.
40. Bacia, K., C. G. Schuette, N. Kahya, R. Jahn, and P. Schwille. 2004. SNAREs prefer liquid-disordered over ''raft'' (liquid-ordered) domains when reconstituted into giant unilamellar vesicles. *J. Biol. Chem.* 279:37951–37955.
41. Vijayendran, R. A., F. S. Ligler, and D. E. Keckband. 1999. A computational reaction-diffusion model for the analysis of transport-limited kinetics. *Anal. Chem.* 71:5405–5412.
42. Schuette, C. G., K. Hatsuzawa, M. Margittai, A. Stein, D. Riedel, P. Kuster, M. Konig, C. Seidel, and R. Jahn. 2004. Determinants of liposome fusion mediated by synaptic SNARE proteins. *Proc. Natl. Acad. Sci. USA.* 101:2858–2863.
43. Laage, R., J. Rohde, B. Brosig, and D. Langosch. 2000. A conserved membrane-spanning amino acid motif drives homomeric and supports heteromeric assembly of presynaptic SNARE proteins. *J. Biol. Chem.* 275:17481–17487.
44. Weninger, K., M. E. Bowen, S. Chu, and A. T. Brunger. 2003. Single-molecule studies of SNARE complex assembly reveal parallel and antiparallel configurations. *Proc. Natl. Acad. Sci. USA.* 100:14800–14805.
45. Wagner, M. L., and L. K. Tamm. 2001. Reconstituted syntaxin1A/SNAP25 interacts with negatively charged lipids as measured by lateral diffusion in planar supported bilayers. *Biophys. J.* 81:266–275.
46. Kweon, D. H., C. S. Kim, and Y. K. Shin. 2003. Regulation of neuronal SNARE assembly by the membrane. *Nat. Struct. Biol.* 10: 440–447.
47. Hu, K., C. Rickman, J. Carroll, and B. Davletov. 2004. A common mechanism for the regulation of vesicular SNAREs on phospholipid membranes. *Biochem. J.* 377:781–785.
48. Hu, K., J. Carroll, S. Fedorovich, C. Rickman, A. Sukhodub, and B. Davletov. 2002. Vesicular restriction of synaptobrevin suggests a role for calcium in membrane fusion. *Nature.* 415:646–650.
49. McNally, J. M., D. J. Woodbury, and J. R. Lemos. 2004. Syntaxin 1A drives fusion of large dense-core neurosecretory granules into a planar lipid bilayer. *Cell Biochem. Biophys.* 41:11–24.
50. Rizo, J. 2003. SNARE function revisited. *Nat. Struct. Biol.* 10: 417–419.
51. Almers, W. 1994. Synapses. How fast can you get? *Nature.* 367: 682–683.
52. von Gersdorff, H., and G. Matthews. 1994. Dynamics of synaptic vesicle fusion and membrane retrieval in synaptic terminals. *Nature.* 367:735–739.